Ground state energy of quantum dots using the coupled cluster method

Winther-Larsen, Sebastian Gregorius[1, *] and Schøyen, Øyvind Sigmundson[1, *]

[1] *University of Oslo*

(Dated: June 8, 2018)

The coupled cluster method for estimating the ground state energy of a many-body system is arguably the most important post-Hartree-Fock method. We have implemented the coupled cluster method with double excitations (CCD). We find that it does not perform well with a simple harmonic oscillator basis, but the results vastly improve when it is provided a basis from a restricted Hatree-Fock self-consistent field method run as a preliminary computation. For a system consisting of $N = 2$ interacting particles, using 12 orbital shells we get a ground stated energy of 3.005970, very close to the analytical "true answer" of 3[1].

CONTENTS

---

* Project code: https://github.com/Schoyen/FYS4411

I. INTRODUCTION

In this project we will compute the ground state energy of quantum dots, a construct that has become a popular area of study in recent decades, both from a theoretical and an experimental point of view. We achieve the ground state computation by implementing a coupled cluster amplitude equation solver which is used in succession with a restricted Hartree-Fock self-consistent field method.

Regardless of how sophisticated the method used, the many-body problem remains quite intractable. The true wavefunction of any system will be a linear combination of all possible slater-type orbitals one can model. This means that in order to represent a system correctly, one would need a basis set of infinite size. This is an obvious problem when we solve problems numerically, because we obviously need to limit the size of the basis we use because we have limitations in memeory and computating power. Luckily, great minds have bestowed a wide selection of very god numerical methods upon the world, which the coupled cluster is a part of.

First, we provide a thorough theoretical outline of how we model a quantum dot, the mathematical formalism behind many-body problems and outline how the computational methods we employ both turn into iterative schemes that are easy to represent numerically. Second, we provide a brief overview of the program we have constructed which is in the form an installable python package. Third, we have employed the methods on a large parameter space presenting results for systems consisting of $N = \{2, 6, 12, 20\}$ particles. Fourth, we discuss the most interesting aspects of the results and try to shed some light over the shortcomings as well as the beneficial features of the different metods. Lastly, we end on some summary remarks.

II. THEORY

In this project we will study a system of N interacting electrons. We will be looking at a Hamiltonian consisting of a one-body and a two-body part. The one-body part is given by

$$h(\mathbf{r}_i) = -\frac{1}{2}\nabla_i^2 + \frac{1}{2}\omega^2\mathbf{r}_i^2, \tag{1}$$

where we use natural units $\hbar = c = e = 1$ and set the mass to unity. The two-body part is the Coulomb interaction potential,

$$u(\mathbf{r}_i, \mathbf{r}_j) = \frac{1}{|\mathbf{r}_i - \mathbf{r}_j|}. \tag{2}$$

We thus get the total Hamiltonian

$$H = h + u = \sum_{i=1}^{N} h(\mathbf{r}_i) + \sum_{i<j}^{N} u(\mathbf{r}_i, \mathbf{r}_j), \tag{3}$$

where h is the full one-body operator and u the full two-body operator, i.e., over the entire system. Working in a basis of L single particle functions, $\{|p\rangle\}_{p=1}^{L}$. We define the reference Slater determinant as

$$|\Phi_0\rangle \equiv |1, 2, \ldots, N\rangle, \tag{4}$$

i.e., a tensorproduct of the N first single particle functions, $|i\rangle$, of the system. We call these single particle functions *occupied* as they are contained in the Slater determinant. We will denote the occupied indices with $i, j, k, l, \cdots \in \{1, \ldots, N\}$, the *virtual* states with $a, b, c, d, \cdots \in \{N+1, \ldots, L\}$ and general indices with $p, q, r, s, \cdots \in \{1, \ldots, L\}$. In terms of sets of basis functions we can write this as

$$\{|p\rangle\}_{p=1}^{L} = \{|i\rangle\}_{i=1}^{N} \cup \{|a\rangle\}_{a=N+1}^{L}, \tag{5}$$

i.e., the general indexed states consists of both occupied and virtual states. Note that the single particle functions are orthonormal, i.e.,

$$\langle p|q\rangle = \delta_{pq}. \tag{6}$$

We can construct other Slater determinants in this basis by exciting or relaxing the reference determinant. A general excitation is labeled $|\Phi_{ij\ldots}^{ab\cdots}\rangle$ which means that we have removed the single particle functions with indices $i, j, \ldots$ from the reference and added $a, b, \ldots$. Note that

$$\langle \Phi_{ij\ldots}^{ab\cdots}|\Phi_0\rangle = 0, \tag{7}$$

for any excitation.

A. *Motivational Interlude*: Quantum Dots

The system described above is a theoretical approximation of a quantum dot. Some consideration should

be given to an explanation of why the system described above is a quantum dot, and why we should care about quantum dots. There are at least two things we refer to as quantum dots. The first one is a man-made device, also known as artificial atoms, and the other is the simplest theoretical construct of such a device.

Aritifical atom quantum dots are semiconducting crystals, typically GaAs, and they are relatively easy to build in a laboratory. Some free electrons are confined to a volume, either by a physical barrier, like an insulator, or an electromagnetic field[2]. Due to the confinement of the electrons, the energy levels of a quantum dot becomes quantized, and they therefore hold many properties similar to naturally occuring quantized systems, which is the reason why quantum dots have attracted much interest.

The theoretical approximation of a quantum dot is impossible to make perfectly accurate, yet simple. There are some important effects that should be included such the potential arising as a result of the confinement, and the interaction between particles. We therefore model our system with an electron-electron interaction, given by the two-body operator in Equation 2, and with we approximate the confining potential by the harmonic oscillator potential, given by the second term in the one-body Hamiltonian in Equation 1. The last term in the one-body Hamiltonian is the kinetic energy of particle in question, essential in any system.

B. Second quantization

Employing the creation operators, $a_p^\dagger$, and the destruction operators, a_p, we can write the Hamiltonian as

$$H = \sum_{pq} h_q^p a_p^\dagger a_q + \frac{1}{4}\sum_{pqrs} \langle pq||rs\rangle a_p^\dagger a_q^\dagger a_s a_r, \tag{8}$$

where the sums are general indices over all L basis states and the matrix elements are defined as

$$h_q^p \equiv \langle p|h|q\rangle, \tag{9}$$
$$\langle pq||rs\rangle \equiv \langle pq|u|rs\rangle - \langle pq|u|sr\rangle. \tag{10}$$

Note that we use the "chemists notation" to label the antisymmetric matrix elements.

C. The coupled cluster approximation

We approximate the true wavefunction, $|\Psi\rangle$, of the system by the coupled cluster wavefunction, $|\Psi_{\text{CC}}\rangle$, defined by

$$|\Psi_{\text{CC}}\rangle \equiv e^T|\Phi_0\rangle = \left(\sum_{i=0}^{n}\frac{1}{n!}T^n\right)|\Phi_0\rangle, \tag{11}$$

where the *cluster operator*, T, is given by a sum of p-excitation operators labeled T_p. They consist of *cluster*

amplitudes, $t_{i\dots}^{a\dots}$, and creation and annihilation operators.

$$T = T_1 + T_2 + \cdots + T_p \tag{12}$$

$$= \sum_{ia} t_i^a a_a^\dagger a_i + \left(\frac{1}{2!}\right)^2 \sum_{ijab} t_{ij}^{ab} a_a^\dagger a_b^\dagger a_i a_j + \dots. \tag{13}$$

In our approximation we limit the cluster operator to only include double excitations,

$$T \equiv T_2 = \frac{1}{4} \sum_{ijab} t_{ij}^{ab} a_a^\dagger a_b^\dagger a_j a_i. \tag{14}$$

The first part of the coupled cluster method consists of constructing the cluster amplitudes using the *amplitude equations*. After we have found the amplitudes we can compute the energy.

D. Energy of the coupled cluster approximation

When we're going to compute the energy of a system using the coupled cluster approximation we would ideally want to find the expectation value of the energy using the coupled cluster wavefunction.

$$E_{\text{CC}} = \langle \Psi_{\text{CC}} | H | \Psi_{\text{CC}} \rangle. \tag{15}$$

As it turns out, this is an uncomfortable way of finding the energy as $T \neq T^\dagger$. Instead we will define what we call the *similarity transformed Hamiltonian*. We plug the coupled cluster wavefunction into the Schrödinger equation.

$$H | \Psi_{\text{CC}} \rangle = E_{\text{CC}} | \Psi_{\text{CC}} \rangle. \tag{16}$$

Next, we left multiply with the inverse of the cluster expansion, i.e.,

$$e^{-T} H | \Psi_{\text{CC}} \rangle = e^{-T} E_{\text{CC}} | \Psi_{\text{CC}} \rangle = E_{\text{CC}} | \Phi_0 \rangle. \tag{17}$$

Projecting this equation on the reference state we get

$$E_{\text{CC}} = \langle \Phi_0 | e^{-T} H | \Psi_{\text{CC}} \rangle = \langle \Phi_0 | e^{-T} H e^{T} | \Phi_0 \rangle, \tag{18}$$

where in the latter inner-product we have located the similarity transformed Hamiltonian defined by

$$\bar{H} \equiv e^{-T} H e^{T}. \tag{19}$$

To simplify the energy equation and the amplitude equations we use the normal ordered Hamiltonian.

$$H = H_N + \langle \Phi_0 | H | \Phi_0 \rangle. \tag{20}$$

The energy equation thus becomes

$$E_{\text{CC}} = \langle \Phi_0 | \bar{H} | \Phi_0 \rangle = E_0 + \langle \Phi_0 | e^{-T} H_N e^{T} | \Phi_0 \rangle, \tag{21}$$

where the reference energy is given by

$$E_0 = \langle \Phi_0 | H | \Phi_0 \rangle. \tag{22}$$

We now define the normal ordered similiarity transformed Hamiltonian as

$$\bar{H}_N \equiv e^{-T} H_N e^{T}. \tag{23}$$

By expanding the exponentials of this Hamiltonian and recognizing the commutators we get the Baker-Campbell-Hausdorff expansion.

$$\bar{H}_N = H_N + [H_N, T] + \frac{1}{2!} \left[[H_N, T], T \right] + \dots. \tag{24}$$

From the connected cluster theorem we know that the only nonzero terms in the Baker-Campbell-Hausdorff expansion will be the terms where the normal ordered Hamiltonian has at least one contraction[1] with every cluster operator on its right. This lets us write the expansion as

$$\bar{H}_N = H_N + (H_N T)_c + \frac{1}{2!} \left(H_N T^2 \right)_c + \dots, \tag{25}$$

where the subscript c signifies that only contributions where at least one contraction between H_N and T has been performed will be included.

1. Coupled cluster doubles energy equation

Using the doubles approximation with the cluster operator T_2 defined in Equation 14 the energy equation becomes

$$E_{\text{CCD}} = E_0 + \langle \Phi_0 | e^{-T_2} H_N e^{T_2} | \Phi_0 \rangle. \tag{26}$$

As the doubles cluster operator doubly excites the reference and using the expansion in Equation 25 we see that we can write the energy equation as

$$E_{\text{CCD}} = E_0 + \langle \Phi_0 | H_N | \Phi_0 \rangle + \langle \Phi_0 | (H_N T_2)_c | \Phi_0 \rangle, \tag{27}$$

as the Hamiltonian is only able to relax one pair of single particle functions. By construction we have that

$$\langle \Phi_0 | H_N | \Phi_0 \rangle = 0. \tag{28}$$

In the second term only the normal ordered two-body operator can contribute as the cluster operator gives a total excitation of $+2$. As we are projecting onto the reference we have to relax to zero again. The normal ordered Fock operator is at most able to excite and relax by 1 and does therefore not contribute to the overall expression.

$$\langle \Phi_0 | (W_N T_2)_c | \Phi_0 \rangle = \frac{1}{4} \sum_{ijab} \langle ij || ab \rangle t_{ij}^{ab}. \tag{29}$$

In total the energy equation reduces to

$$E_{\text{CCD}} = \sum_i h_i^i + \frac{1}{2} \sum_{ij} \langle ij || ij \rangle + \frac{1}{4} \sum_{ijab} \langle ij || ab \rangle t_{ij}^{ab}, \tag{30}$$

where the first two terms come from the reference energy as shown in Equation A10.

———

[1] In the Wick's theorem sense.

E. Coupled cluster amplitude equations

In order for us to solve the energy equation using the coupled cluster approximation we need to figure out what the cluster amplitudes, $t_{ij\ldots}^{ab\ldots}$, are. This is done by projecting Equation 17 onto an excited Slater determinant, i.e.,

$$\langle \Phi_{ij\ldots}^{ab\ldots}|e^{-T}He^{T}|\Phi_0\rangle = 0. \tag{31}$$

Note that in the amplitude equations we can use both the regular and the normal ordered Hamiltonian. They are equal as the reference energy term disappears due to Equation 7. The order of the excitation in the projection determines the order of the amplitudes you will find. In our case we are only interested in the second order ampltiudes found in the doubles approximation, hence we will solve the equation

$$\langle \Phi_{ij}^{ab}|e^{-T}H_N e^{T}|\Phi_0\rangle = 0, \tag{32}$$

to find an expression that can be used to solve for the amplitudes t_{ij}^{ab}. By employing the Baker-Campbell-Haussdorf (BCH) expansion, while setting $T = T_2$, we find

$$\bar{H} = \left(H_N + H_N T_2 + \frac{1}{2}H_N T_2^2\right)_C. \tag{33}$$

The subscript c indicates that only those terms in which the Hamiltonian is connected[2] to every cluster operator on its right should be included. Since the Hamiltonian contains at most four annihilation and creation operators, H_N can connect to at most four cluster operators at once. Therefore, the BCH expansion must truncate at the fourth-order terms.

Now comes the rather tedious task of evaluating all the terms that arises from inserting Equation 33 into Equation 32. This can be done by applying Wick's generalised theorem, but the task is a daunting and streneous one. A few example computations of how this can be done is included in section B. Instead of doing it in this manner, we employ the second quantisation library from SymPy instead[3]. The CCD amplitude equation, from SymPy computation, is

$$\begin{aligned}
0 =&u_{ij}^{ab} + f_c^b t_{ij}^{ac} P(ab) - f_j^k t_{ik}^{ab} P(ij) \\
&+ \frac{1}{4}t_{ij}^{cd} t_{mn}^{ab} u_{cd}^{mn} + \frac{1}{2}t_{ij}^{cd} u_{cd}^{ab} \\
&+ \frac{1}{2}t_{jm}^{cd} t_{in}^{ab} u_{cd}^{mn} P(ij) - \frac{1}{2}t_{nm}^{ac} t_{ij}^{bd} u_{cd}^{nm} P(ab) \\
&+ t_{im}^{ac} t_{jn}^{bd} u_{cd}^{mn} P(ij) + t_{im}^{ac} u_{jc}^{bm} P(ab)P(ij) \\
&- \frac{1}{2}t_{im}^{ab} u_{jn}^{mn}.
\end{aligned} \tag{34}$$

---

[2] Again, in aWick's theorem sense
[3] This is also more in the spirit of this project, as it is within the realm of *Computational* Physics.

1. The Iterative Scheme

At first, we pick only diagonal elements of f to be part of the unperturbed Hamiltonian and consider the rest of the terms a perturbation. The second and third terms in Equation 34 can now be rewritten,

$$\begin{aligned}
f_c^b t_{ij}^{ab} &P(ab) - f_j^k t_{ik}^{ab} P(ij) \\
&\rightarrow f_b^b t_{ij}^{ab} - f_a^a t_{ij}^{ba} - f_j^j t_{ij}^{ab} + f_i^i t_{ji}^{ab} \\
&= (f_a^a + f_b^b - f_i^i - f_j^j) t_{ij}^{ab} \\
&= (\epsilon_a + \epsilon_b - \epsilon_i - \epsilon_j) t_{ij}^{ab} \\
&= -(\epsilon_i + \epsilon_j - \epsilon_a - \epsilon_b) t_{ij}^{ab} \\
&= -D_{ij}^{ab} t_{ij}^{ab}.
\end{aligned} \tag{35}$$

Then we can define a new version of Equation 34,

$$\begin{aligned}
g(u,t) =&u_{ij}^{ab} + \tilde{f}_c^b t_{ij}^{ac} P(ab) - \tilde{f}_j^k t_{ik}^{ab} P(ij) \\
&+ \frac{1}{4}t_{ij}^{cd} t_{mn}^{ab} u_{cd}^{mn} + \frac{1}{2}t_{ij}^{cd} u_{cd}^{ab} \\
&+ \frac{1}{2}t_{jm}^{cd} t_{in}^{ab} u_{cd}^{mn} P(ij) - \frac{1}{2}t_{nm}^{ac} t_{ij}^{bd} u_{cd}^{nm} P(ab) \\
&+ t_{im}^{ac} t_{jn}^{bd} u_{cd}^{mn} P(ij) + t_{im}^{ac} u_{jc}^{bm} P(ab)P(ij) \\
&- \frac{1}{2}t_{im}^{ab} u_{jn}^{mn}.
\end{aligned} \tag{36}$$

where $\tilde{f}$ are the non-diagonal parts of the Fock matrix.

Now we have $D_{ij}^{ab} t_{ij}^{ab} = g(u,t)$. This allows us to define an iterative scheme,

$$t^{(k+1)} = \frac{g(u,t^{(k)})}{D_{ij}^{ab}}, \tag{37}$$

with the initial guess

$$t^{(0)} = \frac{u_{ij}^{ab}}{D_{ij}^{ab}}. \tag{38}$$

2. Intermediate Computations

Looking closely at the amplitude equation in (34) one might come to realize that this equation contains many of the same structures in several of the terms. This warrants the search for an algebraic transformation of the CCD amplitude equation that has the potential to reduce the amount of floating point operations needed to compute it. As it turns out, such terms exist and they will decrease the computing time necessary by an order of magnitude. We will define the following "intermediates",

$$\chi_{cd}^{ab} = \frac{1}{4}t_{mn}^{ab} u_{cd}^{mn} + \frac{1}{2}u_{cd}^{ab} \tag{39}$$

$$\chi_j^n = \frac{1}{2}t_{jm}^{cd} u_{cd}^{mn} \tag{40}$$

$$\chi_d^a = \frac{1}{2}t_{nm}^{ac} u_{cd}^{nm} \tag{41}$$

$$\chi_{jc}^{bm} = u_{jc}^{bm} + \frac{1}{2}t_{jn}^{bd} u_{cd}^{mn} \tag{42}$$

These intermediate structures will allow us to rewrite Equation 34 to,

$$
\begin{aligned}
0 =& u_{ij}^{ab} + f_c^b t_{ij}^{ac} P(ab) - f_j^k t_{ik}^{ab} P(ij) \\
& + t_{ij}^{cd} \chi_{cd}^{ab} + t_{in}^{ab} \chi_j^n P(ij) - t_{ij}^{bd} \chi_d^a P(ab) \\
& + t_{im}^{ac} \chi_{jc}^{bm} P(ab)P(ij) + \frac{1}{2} t_{im}^{ab} u_{jn}^{mn}.
\end{aligned}
\tag{43}
$$

The importance of this "trick" will become apparent in due time.

F. Constructing the matrix elements

Having found the equations needed in order to find an estimate to the ground state energy using the coupled cluster doubles approximation is a well and dandy. But, we need basis functions to create the matrix elements needed to feed into the coupled cluster code. Often these basis functions are not known and we have to use an approximation or utilize Hartree-Fock to create more optimized basis functions.

1. Harmonic oscillator basis

We will be looking at a system of two-dimensional quantum dots with a Coulomb repulsion. If we assume, or make it so, that the repulsive two-body part is small we can use eigenfunctions of the one-body part our basis. In this case we have two-dimensional harmonic oscillator functions as eigenfunctions. We can then compute the matrix elements, h_q^p and u_{rs}^{pq}, before feeding these into the coupled cluster code.

In polar coordinates we can write the harmonic oscillator wavefunction for a single particle in two dimensions as[4].

$$
\phi_{nm}(r,\theta) = N_{nm}(ar)^{|m|} L_n^{|m|}(a^2 r^2) e^{-a^2 r^2/2} e^{im\theta}, \tag{44}
$$

where $a = \sqrt{m\omega/\hbar}$ is the Bohr radius, $L_n^{|m|}$ is the associated Laguerre polynomials, n and m are the principal and azimuthal quantum numbers respectively and N_{nm} is a normalization constant given by

$$
N_{nm} = a\sqrt{\frac{n!}{\pi(n+|m|)!}}. \tag{45}
$$

Included is also the spin, σ, of the wavefunction, which can be either up or down. This means each level, (n,m), is doubly occupied. We also have that the wavefunctions are orthonormal

$$
\langle n_1 m_1 \sigma_1 | n_2 m_2 \sigma_2 \rangle = \delta_{n_1 n_2} \delta_{m_1 m_2} \delta_{\sigma_1 \sigma_2}. \tag{46}
$$

---

[4] Note that this is without spin. As we are looking at fermions this means that each mode of the harmonic oscillator functions will be repeated twice.
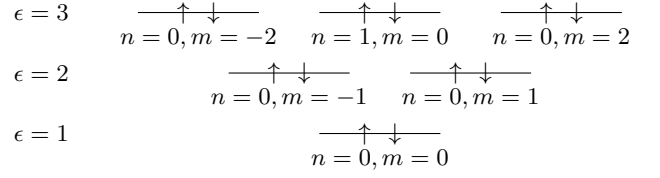

FIG. 1: In this plot we can see the energy degeneracy of the lowest three energy levels in the two-dimensional quantum dot. Each arrow represents a spin up or a spin down state with the quantum numbers n and m as listed below.

The eigenenergy of a single harmonic oscillator is given by

$$
\epsilon_{nm} = \hbar\omega(2n + |m| + 1). \tag{47}
$$

Our next job is now to create a mapping from the three quantum numbers n, m and σ to a single quantum number α as the matrices h and u use single indices for each wavefunction. In Figure 1 we can see the energy levels that needs to be mapped.

Starting from the bottom and working our way upwards from left to right we can label each line from 0 to n in increasing order. This enumeration will serve as our common quantum number α[5]. We will only work with full *shells*, i.e., we restrict our views to systems of N particles where N will be a magic number which we get by counting all spin states for each energy level and the energy levels below. In Figure 1 we can see the magic number $N \in [2, 6, 12]$.

The normalization condition now reads

$$
\langle \alpha | \beta \rangle = \delta_{\alpha\beta} \delta_{\sigma_\alpha \sigma_\beta}, \tag{48}
$$

The one-body matrix will be a diagonal matrix with the eigenenergies of the single particle harmonic oscillator functions as elements.

$$
\langle \alpha | h | \beta \rangle = \epsilon_\beta \delta_{\alpha\beta} \delta_{\sigma_\alpha \sigma_\beta}. \tag{49}
$$

The two-body matrix elements are a little harder to work out as the harmonic oscillator wavefunctions are not eigenfunctions to the correlation operator. Luckily, from E. Anisimovas and A. Matulis (Equation A2)[3] we can get an analytical expression for the two-body matrix elements. We can then construct the antisymmetric two-body matrix elements in the harmonic oscillator basis.

$$
\langle \alpha\beta || \gamma\delta \rangle = \langle \alpha\beta | \gamma\delta \rangle - \langle \alpha\beta | \delta\gamma \rangle. \tag{50}
$$

As we only need to compute these once it is a good idea to save all non-zero values of $\langle \alpha\beta || \gamma\delta \rangle$ to a file.

---

[5] Note that we use greek letters $\alpha, \beta, \dots$ for the harmonic oscillator wavefunctions as opposed to latin letters for the general indices.

2. Constructing the Hartree-Fock basis

Having found the matrix elements of h and u we can now use the *self-consistent field* (SCF) iteration method to construct h and u in a *restricted Hartree-Fock* (RHF) basis. This will yield a better estimate to the actual, unknown basis functions of the system.

The neatest, yet arguably the most abstract, way to write the Hartree-Fock equations for electron i[6] is

$$f_i \varphi_i = \varepsilon_i \varphi_i, \tag{51}$$

where f_i is the Fock operator, φ_i are eigenstates of the Fock operator consiting of a set of one-electorn wave funcitons called the Hartree-Fock molecular orbitals, and ε_i are the eigenenergies of the Fock operator. The fock operator, in matrix notation, is given by

$$F_{pa} = H_{pq} + J(D)_{pq} - \frac{1}{2}K(D)_{pq}, \tag{52}$$

where h_i is the one-body operatore, while the two-body operator is divided into what we call a direct part,

$$J(D)_{pq} = \langle pq|rs \rangle D_{sr}, \tag{53}$$

and an exchange part,

$$K(D)_{pq} = \langle ps|rq \rangle D_{sr}. \tag{54}$$

The direct part of the two-body operator is comparable to classical Coloumb repulsion, while the exchange does not have a classical analog as it arises from the antisymmetry requirement of the wavefunction. D_{sr} is the density matrix of the system.

Introducing a basis set transforms the Hartree-Fock equations into the Rothaan equations

$$FC = SC\varepsilon. \tag{55}$$

This is a generalised eigenvalue problem where S serves as an overlap matrix that must be there in case of non-orthogonal basis. Since the Fock matrix F depends on it's own solution through the orbitals, the eigenvalue problem must be solved iteratively[7]

Because the RHF SCF method is a variational method, the initial wavefunction made up of the single-particle wavefunctions φ_i is varied until the minimal energy is found. The transformations necessary to make all these variations will now be contained in C. So if we start from a harmonic oscillator (HO) basis we can transform into a better basis, called a Hartree-Fock (HF) basis,

$$|\Psi\rangle_p^{\text{HF}} = \sum_{k=1}^{L} C_{kp}|\Psi\rangle_k^{\text{HO}}. \tag{56}$$

We will see how the coupled cluster method with double excitations works with both the HO basis and the HF basis, but not equally well.

---

[6] This is weird, as electron should be indistinguishable and therefore impossible to label.

[7] This is also the reason why the Hartree-Fock-Roothaan equations are often called the self-consistent-field procedure.

III. IMPLEMENTATION

We have costructed a flexible framework for making performing Hartree-Fock self-consistednt field (SCF) and coupled cluster with double excitations (CCD) computations. The entire code base consists of package for python that is easy to install globally on any computer.

Because we have employed a mixture of Python and C++ with Cython interfaces, the code sturcture may be difficult to undertand for someone without Cython experience, but we have tried to make the actual usage of the software as painless as possible.

Most of the computations that are done in a coupled cluster algorithm is linear algebra and we found that NumPy, relying on BLAS and LAPACK, is most likely as fast as it gets and, at the very least, efficient enough for our purposes. The quicker and easier scripting capabilities Python provides is worth what little extra speed-up writing the entire code base in C++ could have provided.

A. Installation and Usage

The software is easy to install by first cloning the GitHub reopsitory,

```
git clone git@github.com:Schoyen/FYS4411.git
```

Then all you need to do is change directory to the project code folder where a MakeFile is included so you only need to build and install,

```
cd FYS4411/project_2/coupled-cluster
make build
make install
```

Now everything should be able to run from anywhere on your computer. To ensure that all requirements of the program are satified you can install with `make installr` instead.

We have included a sample python script in section D that uses almost all methods and classes in the package, and also compares the time each methods takes to fininsh the computations.

B. Program Structure

There are three main subsetions within our program structure, given in the directory tree below.

```
coupled_cluster
├── matrix_elements
│   ├── generate_matrices
│   └── index_map
├── hartree_fock
│   ├── scf_rhf
│   └── basis_transformation
└── schemes
    ├── ccd
    └── ccd_sparse
```

└─ `ccd_optimized`

The first subsection, `matrix_elemtents`, contains methods for computing matrix elements in harmonic oscillator basis from an analytical expression[3]. Computing the matrix elements is a very intensive task, and the central functions are therefore implemented in C++ with a Cython interface to enable use in Python.

The `hartree_fock` subsection contains methods for changing from harmonic oscillator basis to Hartree-Fock basis as well as an implementation of the self-consistent-field algorithm to make this transaction possible.

The `schemes` subsection is arguably the most important part of this project. The subsection has three different classes that perform the exact same computations, but in different and increasingly intelligent ways. First, `CoupledClusterDoubles` is the most straight-forward and naïve way to solve the CCD amplitude equations. Second, because an overbearing amount of the elements in the operator matrices in this problem are zero, we have implemented a sparse matrix CDD solver in `CoupledClusterDoublesSparse`. Third, `CoupledClusterDoublesOptimized` takes advantage of sparse matrices as well, but is also parallellized and optimized with memory use and number of floating point operations in mind.

Both in `CoupledClusterDoublesSparse` and `CoupledClusterDoublesOptimized` we make use of the intermediates in equations 39 to 42. We have also relied upon implementations in C++ for some of the heaviest computations. In the optimized class special care was taken to ensure that every contraction was computed in an optimal way, with the minimization of memory use and CPU time as the overall goal. Moreover, several methods in NumPy for doing linear algebra was tested, including but not limited to `numpy.einsum()`, `numpy.tensordot`, and reshaping datastructures to two dimensions and using `numpy.dot`. Additionally, we tried to make use of the python package `dask` which allows for arrays that are larger than the computer's memory buffer as well as automated concurrency. We found that the dask arrays was a bad fit for our code base, but we ended up using `numba` for automated paralellization of some iterative loops as well as just-in-time compialtion of some functions.

C. Convergence Problems and Mixing

Iterative many-body methods are prone to convergence problems for some configurations. Since Hartree-Fock is a variational method, SCF convergence is found when the energy is stationary with respect to inifitesimal variations in the orbitals. Unfortunately, the SCF iteration scheme does not always converge. Luckily, numerous techniques exist for controlling and accelerating convergence[4]. The same kind of methods have proven useful to ensure convergence of coupled cluster methods [5].

The simplest way to try to "massage" convergence out of the CCD-method is to use *damping* where you include a part of the result from the previous iteration i.e.,

$$\tilde{t}^{k+1} = \theta t^{k+1} + (1-\theta)t^k, \tag{57}$$

where t^{k+1} is the current value computed using Equation 37 and t^k is the previous value for the amplitude. Choosing $\theta \in [0, 1]$ we can tune how much of the previous amplitude we wish to include in the new state. This allows for a more gradual transition between the iterations. We now use $\tilde{t}^{k+1}$ as our estimate of the new amplitude.

A more sophisticated mixing method is the direct inversion in the iterative subspace (DIIS), also known as Pulay mixing. While the common mixing method is used for many other applications [8], the DIIS method is developed with the sole intent of accelerating convergense in Hartree-Fock methods. In DIIS one would construct a linear combinations of approximate errors from previous iterations, analogous to a very clever weighted moving average. We have not implemented this scheme, but it nevertheless warrants mention.

IV. RESULTS

A. Ground state energies for two-dimensional quantum dots

Here we show the ground state energies for the two-dimensional quantum dots using restriced Hartree-Fock (RHF), coupled cluster doubles using both the harmonic oscillator basis and the Hartree-Fock basis which we construct after running the RHF-method. We have chosen the convergence criteria to be 1×10^{-6} in our results for the sake of comparison with M. P. Lohne[6].

All the results from our simulations are displayed in tables I, II, III and IV. They show the ground state energy as a result of restricted Hartree-Fock SCF iterations, and coupled cluster doubles with harmonic oscillator basis and Hatree-Fock basis for systems of increasing size, $N = 2$, $N = 6$, $N = 12$ and $N = 20$ particles respectively. The results are thoroughtly discussed in the next section.

B. Running time

Here we show how the three implementations of the CCD-method scales as a function of the shell number R for $N = 2$ and $N = 6$, in table 2 and 3 respectively. The same behaviour is shown for higher number of particles. In Figure 4 we have plotted the computation time for $N = 6$ particles again, but we have excluded the naïve method for better comparison of the sparse and optimized method.

─────────

[8] It is, for instance, called an alpha filter in data acquisition.

TABLE I: Results for $N = 2$ particles, where convergence was achieved for all parameters. Taut's[1] analytic result for $\omega = 1.0$ a.u. is 3.

ω	R	RHF	CCD(HO)	CCD(HF)
0.1	1	0.596333	0.596333	0.596333
	2	0.596333	0.512520	0.512520
	3	0.526903	0.505972	0.442235
	4	0.526903	0.499216	0.442011
	5	0.525666	0.497172	0.443293
	6	0.525666	0.494232	0.443145
	7	0.525635	0.493142	0.443056
	8	0.525635	0.491895	0.442981
	9	0.525635	0.491262	0.442927
	10	0.525635	0.490649	0.442886
	11	0.525635	0.490262	0.442853
	12	0.525635	0.489918	0.442827
0.5	1	1.886227	1.886227	1.886227
	2	1.886227	1.786914	1.786914
	3	1.799856	1.778903	1.681979
	4	1.799856	1.760117	1.673881
	5	1.799748	1.754385	1.670053
	6	1.799748	1.748232	1.667804
	7	1.799745	1.745231	1.666474
	8	1.799745	1.742548	1.665494
	9	1.799743	1.740860	1.664805
	10	1.799743	1.739444	1.664270
	11	1.799742	1.738416	1.663856
	12	1.799742	1.737562	1.663522
1.0	1	3.253314	3.253314	3.253314
	2	3.253314	3.152328	3.152328
	3	3.162691	3.141827	3.039048
	4	3.162691	3.118679	3.025273
	5	3.161921	3.110967	3.017944
	6	3.161921	3.103338	3.013923
	7	3.161909	3.099324	3.011405
	8	3.161909	3.095916	3.009621
	9	3.161909	3.093662	3.008343
	10	3.161909	3.091818	3.007357
	11	3.161909	3.090436	3.006590
	12	3.161909	3.089299	3.005970
2.0	1	5.772454	5.772454	5.772454
	2	5.772454	5.671234	5.671234
	3	5.679048	5.658272	5.553528
	4	5.679048	5.631669	5.534333
	5	5.677282	5.622092	5.523490
	6	5.677282	5.613118	5.517552
	7	5.677206	5.608130	5.513709
	8	5.677206	5.604026	5.511012
	9	5.677204	5.601216	5.509050
	10	5.677204	5.598946	5.507540
	11	5.677204	5.597213	5.506356
	12	5.677204	5.595791	5.505399

TABLE II: Results for $N = 6$ particles. No convergence is marked as 💀 in the table. For low frequencies the CCD-method using the HO basis has a hard time achieving convergence.

ω	R	RHF	CCD(HO)	CCD(HF)
0.1	2	4.864244	4.864244	4.864244
	3	4.435740	4.446235	4.319901
	4	4.019787	4.383692	3.829962
	5	3.963149	💀	3.666722
	6	3.870617	💀	3.597876
	7	3.863135	💀	3.590388
	8	3.852880	💀	3.587711
	9	3.852591	💀	3.587291
	10	3.852393	💀	3.587136
	11	3.852391	💀	3.586821
	12	3.852382	💀	3.586582
0.5	2	13.640713	13.640713	13.640713
	3	13.051620	13.385987	12.901520
	4	12.357471	13.261097	12.057345
	5	12.325128	13.138572	11.934988
	6	12.271499	13.084158	11.864098
	7	12.271375	13.068399	11.849762
	8	12.271361	13.055561	11.841330
	9	12.271337	13.045386	11.835470
	10	12.271326	13.037878	11.831351
	11	12.271324	💀	11.828242
	12	12.271320	💀	11.825835
1.0	2	22.219813	22.219813	22.219813
	3	21.593198	21.974675	21.423811
	4	20.766919	21.854191	20.429265
	5	20.748402	21.793624	20.332454
	6	20.720257	21.750091	20.274013
	7	20.720132	21.718843	20.249849
	8	20.719248	21.695224	20.234705
	9	20.719248	21.675931	20.224389
	10	20.719217	21.661830	20.217075
	11	20.719215	21.649812	20.211541
	12	20.719215	21.640765	20.207258
2.0	2	37.281425	37.281425	37.281425
	3	36.637217	37.042127	36.450634
	4	35.689555	36.925664	35.328432
	5	35.681729	36.864367	35.250185
	6	35.672333	36.812895	35.200308
	7	35.671851	36.775986	35.168245
	8	35.670358	36.747864	35.147097
	9	35.670333	36.725261	35.131953
	10	35.670144	36.708362	35.121033
	11	35.670143	36.694188	35.112680
	12	35.670127	36.683281	35.106188

V. DISCUSSION

A. Performance comparison

Somewhat surprisingly, the Hartree-Fock method outperforms the coupled cluster doubles when the harmonic oscillator basis is used. This happens for almost any configuration except the smallest system with $N = 2$ particles. This comes from the fact that the HO basis is not very good at representing the states in the system. As we have already stated, because the Hartree-Fock SCF iterations is a variational methhod, the basis is varied in order to find the minimal energy. The new basis states will be linear combinations of the old basis states. When the iterations are finished, the new transformed HF basis will

TABLE III: Here we look at $N = 12$ particles ($R = 3$ shells). We did not achieve convergence using the harmonic oscillator basis for the lower frequency values and large number of shells. No convergence is marked as ☠ in the table.

ω	R	RHF	CCD(HO)	CCD(HF)
	3	46.361130	46.361130	46.361130
	4	43.663267	45.837079	43.309845
	5	41.108851	45.456883	40.654710
	6	40.750512	☠	40.068340
0.5	7	40.302719	☠	39.508500
	8	40.263752	☠	39.399128
	9	40.216688	☠	39.329311
	10	40.216252	☠	39.309409
	11	40.216195	☠	39.296007
	12	40.216165	☠	39.285968
	3	73.765549	73.765549	73.765549
	4	70.673849	73.314476	70.324250
	5	67.569930	72.990679	67.031096
	6	67.296869	☠	66.526677
1.0	7	66.934745	☠	66.049564
	8	66.923094	☠	65.972157
	9	66.912244	☠	65.921205
	10	66.912035	☠	65.889281
	11	66.911365	☠	65.866715
	12	66.911364	☠	65.849776
	3	120.722260	120.722260	120.722260
	4	117.339642	120.296556	116.995036
	5	113.660396	120.007146	113.048934
	6	113.484866	119.759037	112.658821
2.0	7	113.247601	119.662199	112.309482
	8	113.246579	119.584733	112.235521
	9	113.246303	119.524394	112.181828
	10	113.245854	119.472283	112.140661
	11	113.245256	119.430353	112.109973
	12	113.245183	119.394712	112.085683
	3	242.334879	242.334879	242.334879
	4	238.739591	241.927593	238.394598
	5	234.352741	241.663950	233.680649
	6	234.282331	241.507595	233.425243
5.0	7	234.194820	241.390525	233.226529
	8	234.194059	241.293417	233.137933
	9	234.190797	241.221056	233.070205
	10	234.190714	241.158896	233.020009
	11	234.190665	241.109926	232.980634
	12	234.190553	241.068091	232.948528

TABLE IV: In this table we look at $N = 20$ particles ($R = 4$ shells). We did not achieve convergence using the harmonic oscillator basis for the lower frequency values and large number of shells. No convergence is marked as ☠ in the table.

ω	R	RHF	CCD(HO)	CCD(HF)
	4	177.963297	177.963297	177.963297
	5	168.792442	177.206536	168.459124
	6	161.339721	☠	160.594507
	7	159.958722	☠	158.841120
1.0	8	158.400172	☠	157.038330
	9	158.226030	☠	156.676039
	10	158.017667	☠	156.367930
	11	158.010276	☠	156.292422
	12	158.004951	☠	156.238258
	4	286.825295	286.825295	286.825295
	5	276.898196	286.159148	276.381708
	6	267.269712	285.614958	266.413122
	7	266.213200	☠	264.969415
2.0	8	264.933622	☠	263.434546
	9	264.874009	☠	263.215451
	10	264.809954	☠	263.046195
	11	264.809901	☠	262.963703
	12	264.809306	☠	262.899698
	4	563.773952	563.773952	563.773952
	5	552.630093	563.160136	552.118708
	6	540.804720	562.692231	539.824400
	7	540.227793	562.306123	538.886074
5.0	8	539.499326	562.114279	537.925127
	9	539.495941	☠	537.769045
	10	539.494611	☠	537.646668
	11	539.493513	☠	537.548828
	12	539.491764	☠	537.470616
	4	973.032700	973.032700	973.032700
	5	961.371081	972.439478	960.862053
	6	948.057077	972.002302	947.019789
	7	947.765474	971.716015	946.399546
10.0	8	947.410305	971.508584	945.827806
	9	947.409440	971.332133	945.663820
	10	947.404930	971.193592	945.528489
	11	947.404361	971.076617	945.424175
	12	947.403875	970.978571	945.339080

B. Validity of results

The analytical computed energy for $\omega = 1.0$ a.u. and $N = 2$ is 3[1]. From our tables we see that RHF is least successful in reaching this value, CCD in HF basis is best, while CCD with HO basis is generally somewhere between the two. We see that we get even closer to the analytical "truth" by increasing the number of shells.

The rest of results have been compared with the master thesis of M. P. Lohne[7] for up to 10 shells. Lohne gets two sets of energies, one set from RHF and one set from CCSD code with harmonic oscillator basis functions. Our CCD code with Hartree-Fock basis will for some configu-
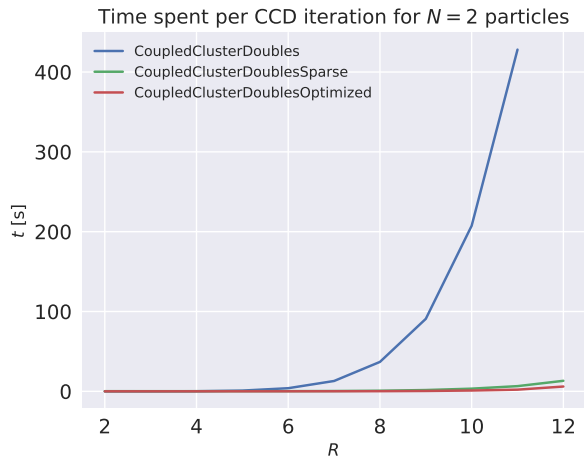
then be much better at representing the possible quantum configurations compared to the HO basis. This effect is only apparent in system with a larger number of particles and/or low frequency. This is because in a system with a large number of particles relative to the frequency particle-particle interaction will be more prominent than the harmonic oscillator potential the particles are subject to. I other words, the HO basis would fit rather well.

FIG. 2: In this figure we can see the running time per iteration for $N = 2$ particles as a function of the shell number R. We did not run the naïve implementation for $R = 12$.
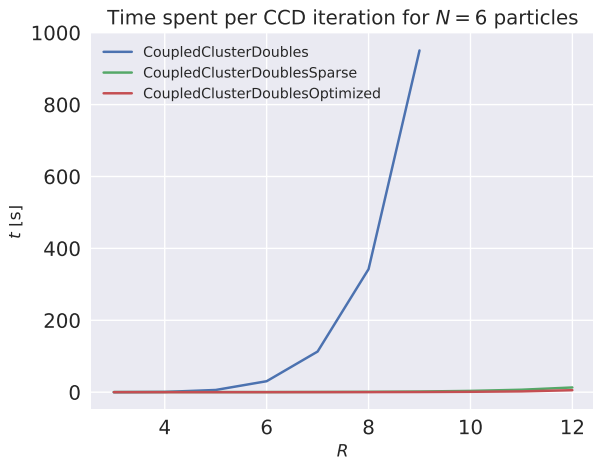

FIG. 3: Here we see the running time per iteration for $N = 6$ particles as a function of the shell number R. We did not run the naïve implementation for $R > 9$ in this figure.

rations[9] beat CCSD with plain harmonic oscillator basis. For 12 shells we can compare with the results from M. P. Lohne et al.[6], but in this article an *effective interaction* for the Hamiltonian with a CCSD code has been used. These results are therefore significanlty better than ours, but we can get a "ball-park" idea to benchmark against.

———————

[9] By configurations we mean frequency ω and number of particles N.
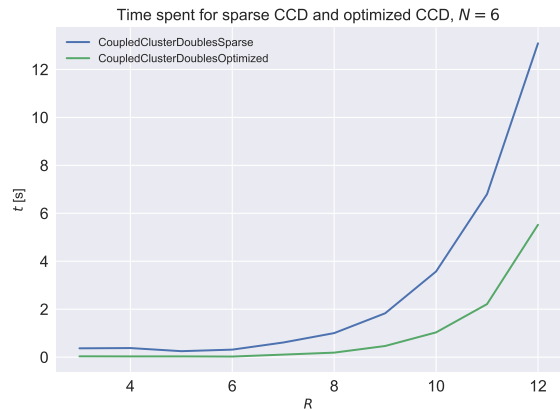
FIG. 4: Run time for $N = 6$ particles, only the faster methods are included for better comparison.

C. Running time

Looking at the running times shown in Figure 2 and Figure 3 we can see how the naïve implementation blows up very fast. As both the sparse and the optimized version uses intermediate calculations these running times scales on the order of $\mathcal{O}(l^6)$ whereas the naïve implementation goes as $\mathcal{O}(l^8)$. Another important factor is that the naïve implementation uses `np.einsum` to calculate the tensor contractions whereas the sparse and optimized version uses `sparse.tensordot` and `np.matmul` respectively. The two latter function calls uses BLAS's implementation of the matrix dot which is way faster than Numpys `np.einsum`.

D. Convergence trouble

For a large number of particles and a low frequency the CCD-method get trouble with convergence. This happens as the confining potential $v \propto \omega^2$ will not be able to confine the particles when the interaction gets too strong. The CCD-method will in particular get a hard time keep the particles together as the excitation operator t only excites pairs of particles leading to a too strong increase in the interaction when the particles increase their energy level. This effect can potentially be somewhat alleviated by including the singles excitation, e.g., using the CCSD-method.

We can see this behaviour in our results. For $N = 2$ we get convergence for all methods for $\omega = 0.1$ shown in Table I. By increasing to $N = 6$ particles we immediately see how CCD with the HO basis will get in trouble for small values of ω. Even by increasing the strength of the confinement this method does converge.

For $N = 6$ none of the methods converged when

$\omega = 0.1^{10}$. By increasing the frequency we restored the convergence. For larger number of shells we had to start increasing the value of $\theta \to 0.9$ in order to get convergence within the threshold.

CCD with HO basis experiences the same convergence problems also for, $N = 12$ particles and for $N = 20$ particles.

VI.   SUMMARY REMARKS

Our main product from this is a product that can do both computations with restricted Hartree-Fock (RHF) self-consistent field and coupled cluster doubles (CCD). We have tried to make a package in python that should be easy enough for anyone to test. Moreover we hav demonstrated that one can speed up the computation time with a relatively simple algebraic transformation and finding the "intermediates". The computational speed was further reduced using sparse matrices. It should be noted, as a warning, that there are relatively few systems adequately sparse for this to work. We added upon the program to increase it further with paralellization and optimal use of numerical functions.

In order to perform the computations we have constructed a harmonic oscillator basis. We saw how the CCD method was outperformed RHF in most cases, and often exhibited convergence problems. The remedy for these shortcomings is to use the Hartree-Fock basis which is provided after successful convergence of SCF iterations. The results are improved markedly and classification of coupled cluster methods as a post-Harte-Fock method is justified.

The coupled cluster method provides surprisingly good results even though one only includes double esctiations. The reason for this is that particle-particle interactions is the amongst the most important thing that happens in a ferminon system, second only to no interaction at all, i.e what particles do on their own. The way to improve the computations is to include other types of excitations like singles (CCSD) and triples (CCSDT), add more basis functions, and/or supplement the coupled cluster method with another method like a perturbative one. All of this will, needless to say, increase the compute time, which must be balanced against the accuracy needed for the situation at hand.

Appendix A: The normal ordered Hamiltonian

When constructing the normal ordered Hamiltonian we use Wick's theorem to write the one-body, h, and the two-body, u, operators onto a normal ordered form. Specifically we define the normal ordered form in terms of the *Fermi vacuum*[11]. That is, an operator on normal ordered form destroys the reference Slater determinant.

We start by writing the one-body operator, h, to its normal-ordered form.

$$h = \sum_{pq} h_q^p a_p^\dagger a_q = \sum_{pq} h_q^p \left(\{a_p^\dagger a_q\} + \{\overline{a_p^\dagger a_q}\} \right) \quad \text{(A1)}$$

$$= \sum_{pq} h_q^p \{a_p^\dagger a_q\} + \sum_{pq} h_q^p \delta_{p\in i} \delta_{pq} \quad \text{(A2)}$$

$$= h_N + \sum_i h_i^i, \quad \text{(A3)}$$

where we have used $\delta_{p\in i}$ to mean that p must be an occupied index. Doing the same for the two-body operator is a slightly more tedious endeavor. For brevity we will only write out the operator strings and only keep the non-zero contributions.

$$a_p^\dagger a_q^\dagger a_s a_r = \{a_p^\dagger a_q^\dagger a_s a_r\} + \{\overline{a_p^\dagger a_q^\dagger} a_s a_r\} + \{\overline{a_p^\dagger a_q^\dagger a_s a_r}\}$$
$$+ \{a_p^\dagger \overline{a_q^\dagger} a_s a_r\} + \{a_p^\dagger \overline{a_q^\dagger a_s} a_r\}$$
$$+ \{\overline{a_p^\dagger a_q^\dagger a_s a_r}\} + \{\overline{a_p^\dagger a_q^\dagger a_s a_r}\} \quad \text{(A4)}$$
$$= \{a_p^\dagger a_q^\dagger a_s a_r\} - \delta_{p\in i} \delta_{ps} \{a_q^\dagger a_r\} + \delta_{p\in i} \delta_{pr} \{a_q^\dagger a_s\}$$
$$+ \delta_{q\in i} \delta_{qs} \{a_p^\dagger a_r\} - \delta_{q\in i} \delta_{qr} \{a_p^\dagger a_s\}$$
$$- \delta_{p\in i} \delta_{ps} \delta_{q\in j} \delta_{qr} + \delta_{p\in i} \delta_{pr} \delta_{q\in j} \delta_{qs}. \quad \text{(A5)}$$

Inserted into the full two-body operator and sorting out the sums we get

$$u = \frac{1}{4} \sum_{pqrs} \langle pq||rs \rangle \{a_p^\dagger a_q^\dagger a_s a_r\} - \frac{1}{4} \sum_{iqr} \langle iq||ri \rangle \{a_q^\dagger a_r\}$$
$$+ \frac{1}{4} \sum_{iqs} \langle iq||is \rangle \{a_q^\dagger a_s\} + \frac{1}{4} \sum_{pir} \langle pi||ri \rangle \{a_p^\dagger a_r\}$$
$$- \frac{1}{4} \sum_{pis} \langle pi||is \rangle \{a_p^\dagger a_s\} - \frac{1}{4} \sum_{ij} \langle ij||ji \rangle$$
$$+ \frac{1}{4} \sum_{ij} \langle ij||ij \rangle. \quad \text{(A6)}$$

Using the antisymmetric properties of the two-body matrix elements,

$$\langle pq||rs \rangle = -\langle pq||sr \rangle = -\langle qp||rs \rangle = \langle qp||sr \rangle, \quad \text{(A7)}$$

---

[10] The RHF-method would probably have converged if we had started tuning its mixing parameter, but as we have focused on CCD we did not think it relevant to include these results.

[11] Fermi vacuum defines the reference state, i.e., $|\Phi_0\rangle$, as the vacuum.

and relabeling of the indices we can rearrange and collect some terms.

$$u = W_N + \sum_{pir}\langle pi||ri\rangle\{a_p^\dagger a_r\} + \frac{1}{2}\sum_{ij}\langle ij||ij\rangle, \quad \text{(A8)}$$

where the normal ordered two-body operator is

$$W_N = \frac{1}{4}\sum_{pqrs}\langle pq||rs\rangle\{a_p^\dagger a_q^\dagger a_s a_r\}. \quad \text{(A9)}$$

When we now construct the full Hamiltonian we can collect some terms. The constants in both the one-body and the two-body operator in total constitues the reference energy.

$$E_0 \equiv \langle\Phi_0|H|\Phi_0\rangle = \sum_i h_i^i + \frac{1}{2}\sum_{ij}\langle ij||ij\rangle. \quad \text{(A10)}$$

Combining the normal ordered one-body operator and the second term in the two-body operator, i.e., the term with a single creation and annihilation operator pair, we get the normal ordered Fock-operator.

$$F_N = \sum_{pq} h_q^p\{a_p^\dagger a_q\} + \sum_{pqi}\langle pi||qi\rangle\{a_p^\dagger a_q\} \quad \text{(A11)}$$

$$= \sum_{pq} f_q^p\{a_p^\dagger a_q\}, \quad \text{(A12)}$$

where we have defined the Fock matrix elements as

$$f_q^p = h_q^p + \sum_i\langle pi||qi\rangle. \quad \text{(A13)}$$

In total we get the full Hamiltonian

$$H = F_N + W_N + \langle\Phi_0|H|\Phi_0\rangle \quad \text{(A14)}$$

$$= H_N + \langle\Phi_0|H|\Phi_0\rangle, \quad \text{(A15)}$$

which is what we wanted to show.[8]

Appendix B: Amplitude Equations

In this section we have provided a few sample computations of how one would evaluate the amplitude equations using wicks theorem. Starting with the simplest term including only the normal-ordered Hamiltonian,

$$\langle\Phi_{ij}^{ab}|(F_N + V_N)|\Phi_0\rangle$$
$$= \sum_{pq} f_{pq}\langle\Phi_0|\{a_i^\dagger a_j^\dagger a_b a_a\}\{a_p^\dagger a_q\}|\Phi_0\rangle$$
$$+ \frac{1}{4}\sum_{pqrs}\langle pq||rs\rangle\langle\Phi_0|\{a_i^\dagger a_j^\dagger a_b a_a\}\{a_p^\dagger a_q^\dagger a_s a_r\}|\Phi_0\rangle. \quad \text{(B1)}$$

The one-electron component does not have any full contractions, while the two-electron component produces one contributing integral,

$$\langle\Phi_{ij}^{ab}|(V_N)|\Phi_0\rangle$$
$$= \frac{1}{4}\sum_{pqrs}\langle pq||rs\rangle\langle\Phi_0|\{a_i^\dagger a_j^\dagger a_b a_a\}\{a_p^\dagger a_q^\dagger a_s a_r\}|\Phi_0\rangle$$
$$= \frac{1}{4}\sum_{pqrs}\langle pq||rs\rangle$$
$$\times \Big(\{a_i^\dagger a_j^\dagger a_b a_a a_p^\dagger a_q^\dagger a_s a_r\} + \{a_i^\dagger a_j^\dagger a_b a_a a_p^\dagger a_q^\dagger a_s a_r\}$$
$$+ \{a_i^\dagger a_j^\dagger a_b a_a a_p^\dagger a_q^\dagger a_s a_r\} + \{a_i^\dagger a_j^\dagger a_b a_a a_p^\dagger a_q^\dagger a_s a_r\} \Big)$$
$$= \frac{1}{4}\sum_{pqrs}\langle pq||rs\rangle(\delta_{ap}\delta_{bq}\delta_{js}\delta_{ir} - \delta_{aq}\delta_{bp}\delta_{js}\delta_{ir}$$
$$- \delta_{ap}\delta_{bq}\delta_{jr}\delta_{is} + \delta_{aq}\delta_{bp}\delta_{jr}\delta_{is})$$
$$= \langle ab||ij\rangle = u_{ij}^{ab}. \quad \text{(B2)}$$

Next we would like to evaluate $\langle\Phi_{ij}^{ab}|(F_N + V_N)T_2|\Phi_0\rangle$. Starting with the term involving the Fock operator F_N,

$$\langle\Phi_{ij}^{ab}|F_N T_2|\Phi_0\rangle$$
$$= \frac{1}{4}\sum_{pq}\sum_{klcd} f_{pq}t_{kl}^{cd}\langle\Phi_0|\{a_i^\dagger a_j^\dagger a_b a_a\}(\{a_p^\dagger a_q\}\{a_c^\dagger a_d^\dagger a_l a_k\})_c|\Phi_0\rangle$$
$$= \frac{1}{4}\sum_{pq}\sum_{klcd} f_{pq}t_{kl}^{cd}$$
$$\times \Big(\{a_i^\dagger a_j^\dagger a_b a_a a_p^\dagger a_q a_c^\dagger a_d^\dagger a_l a_k\} + \{a_i^\dagger a_j^\dagger a_b a_a a_p^\dagger a_q a_c^\dagger a_d^\dagger a_l a_k\}$$
$$+ \{a_i^\dagger a_j^\dagger a_b a_a a_p^\dagger a_q a_c^\dagger a_d^\dagger a_l a_k\} + \{a_i^\dagger a_j^\dagger a_b a_a a_p^\dagger a_q a_c^\dagger a_d^\dagger a_l a_k\}$$
$$+ \{a_i^\dagger a_j^\dagger a_b a_a a_p^\dagger a_q a_c^\dagger a_d^\dagger a_l a_k\} + \{a_i^\dagger a_j^\dagger a_b a_a a_p^\dagger a_q a_c^\dagger a_d^\dagger a_l a_k\}$$
$$+ \{a_i^\dagger a_j^\dagger a_b a_a a_p^\dagger a_q a_c^\dagger a_d^\dagger a_l a_k\} + \{a_i^\dagger a_j^\dagger a_b a_a a_p^\dagger a_q a_c^\dagger a_d^\dagger a_l a_k\}$$
$$+ \{a_i^\dagger a_j^\dagger a_b a_a a_p^\dagger a_q a_c^\dagger a_d^\dagger a_l a_k\} + \{a_i^\dagger a_j^\dagger a_b a_a a_p^\dagger a_q a_c^\dagger a_d^\dagger a_l a_k\}$$
$$+ \{a_i^\dagger a_j^\dagger a_b a_a a_p^\dagger a_q a_c^\dagger a_d^\dagger a_l a_k\} + \{a_i^\dagger a_j^\dagger a_b a_a a_p^\dagger a_q a_c^\dagger a_d^\dagger a_l a_k\}$$
$$+ \{a_i^\dagger a_j^\dagger a_b a_a a_p^\dagger a_q a_c^\dagger a_d^\dagger a_l a_k\} + \{a_i^\dagger a_j^\dagger a_b a_a a_p^\dagger a_q a_c^\dagger a_d^\dagger a_l a_k\}$$
$$+ \{a_i^\dagger a_j^\dagger a_b a_a a_p^\dagger a_q a_c^\dagger a_d^\dagger a_l a_k\} + \{a_i^\dagger a_j^\dagger a_b a_a a_p^\dagger a_q a_c^\dagger a_d^\dagger a_l a_k\} \Big) \quad \text{(B3)}$$

$$
\begin{aligned}
=&\sum_{pq}\sum_{klcd}f_{pq}t_{kl}^{cd}\\
\times&(-\delta_{ac}\delta_{bd}\delta_{ik}\delta_{jq}\delta_{lp}+\delta_{ac}\delta_{bd}\delta_{il}\delta_{jq}\delta_{kp}\\
&+\delta_{ac}\delta_{bd}\delta_{iq}\delta_{jk}\delta_{lp}-\delta_{ac}\delta_{bd}\delta_{iq}\delta_{jl}\delta_{kp}\\
&+\delta_{ac}\delta_{bp}\delta_{dq}\delta_{ik}\delta_{jl}-\delta_{ac}\delta_{bp}\delta_{dq}\delta_{il}\delta_{jk}\\
&+\delta_{ad}\delta_{bc}\delta_{ik}\delta_{jq}\delta_{lp}-\delta_{ad}\delta_{bc}\delta_{il}\delta_{jq}\delta_{kp}\\
&-\delta_{ad}\delta_{bc}\delta_{iq}\delta_{jk}\delta_{lp}+\delta_{ad}\delta_{bc}\delta_{iq}\delta_{jl}\delta_{kp}\\
&-\delta_{ad}\delta_{bp}\delta_{cq}\delta_{ik}\delta_{jl}+\delta_{ad}\delta_{bp}\delta_{cq}\delta_{il}\delta_{jk}\\
&-\delta_{ap}\delta_{bc}\delta_{dq}\delta_{ik}\delta_{jl}+\delta_{ap}\delta_{bc}\delta_{dq}\delta_{il}\delta_{jk}\\
&+\delta_{ap}\delta_{bd}\delta_{cq}\delta_{ik}\delta_{jl}-\delta_{ap}\delta_{bd}\delta_{cq}\delta_{il}\delta_{jk})\\
=&(f_{bc}t_{ij}^{ac}-f_{ac}t_{ij}^{bc})-(f_{jk}t_{ik}^{ab}-f_{ik}t_{jk}^{ab})\\
=&f_{bc}t_{ij}^{ac}P(ab)-f_{kj}t_{ik}^{ab}P(ij)
\end{aligned}
\tag{B4}
$$

Where in the last steps we have consigned the sums by Einstein summation notation.

Appendix C: Finding Amplitude Equation Intermediates

Starting from the CCD amplitude equation we factor out terms that will have the same indices if we contract them,

$$
\begin{aligned}
0=&u_{ij}^{ab}+f_c^bt_{ij}^{ac}P(ab)-f_j^kt_{ik}^{ab}P(ij)\\
&+\frac{1}{4}t_{ij}^{cd}t_{mn}^{ab}u_{cd}^{mn}+\frac{1}{2}t_{ij}^{cd}u_{cd}^{ab}\\
&+\frac{1}{2}t_{jm}^{cd}t_{in}^{ab}u_{cd}^{mn}P(ij)-\frac{1}{2}t_{nm}^{ac}t_{ij}^{bd}u_{cd}^{nm}P(ab)\\
&+t_{im}^{ac}t_{jn}^{bd}u_{cd}^{mn}P(ij)+t_{im}^{ac}u_{jc}^{bm}P(ab)P(ij)\\
&+\frac{1}{2}t_{im}^{ab}u_{jn}^{mn},
\end{aligned}
\tag{C1}
$$

$$
\begin{aligned}
0=&u_{ij}^{ab}+f_c^bt_{ij}^{ac}P(ab)-f_j^kt_{ik}^{ab}P(ij)\\
&+t_{ij}^{cd}\left(\frac{1}{4}t_{mn}^{ab}u_{cd}^{mn}+\frac{1}{2}u_{cd}^{ab}\right)\\
&+t_{in}^{ab}\left(\frac{1}{2}t_{jm}^{cd}u_{cd}^{mn}\right)P(ij)\\
&-t_{ij}^{bd}\left(\frac{1}{2}t_{nm}^{ac}u_{cd}^{nm}\right)P(ab)\\
&+\frac{1}{2}t_{im}^{ac}t_{jn}^{bd}u_{cd}^{mn}P(ij)-\frac{1}{2}t_{im}^{bc}t_{jn}^{ad}u_{cd}^{mn}P(ij)\\
&+t_{im}^{ac}u_{jc}^{bm}P(ab)P(ij)\\
&+\frac{1}{2}t_{im}^{ab}u_{jn}^{mn}
\end{aligned}
\tag{C2}
$$

$$
\begin{aligned}
0=&u_{ij}^{ab}+f_c^bt_{ij}^{ac}P(ab)-f_j^kt_{ik}^{ab}P(ij)\\
&+t_{ij}^{cd}\left(\frac{1}{4}t_{mn}^{ab}u_{cd}^{mn}+\frac{1}{2}u_{cd}^{ab}\right)\\
&+t_{in}^{ab}\left(\frac{1}{2}t_{jm}^{cd}u_{cd}^{mn}\right)P(ij)\\
&-t_{ij}^{bd}\left(\frac{1}{2}t_{nm}^{ac}u_{cd}^{nm}\right)P(ab)\\
&+\frac{1}{2}t_{im}^{ac}t_{jn}^{bd}u_{cd}^{mn}P(ab)P(ij)\\
&+t_{im}^{ac}u_{jc}^{bm}P(ab)P(ij)\\
&+\frac{1}{2}t_{im}^{ab}u_{jn}^{mn}
\end{aligned}
\tag{C3}
$$

$$
\begin{aligned}
0=&u_{ij}^{ab}+f_c^bt_{ij}^{ac}P(ab)-f_j^kt_{ik}^{ab}P(ij)\\
&+t_{ij}^{cd}\left(\frac{1}{4}t_{mn}^{ab}u_{cd}^{mn}+\frac{1}{2}u_{cd}^{ab}\right)\\
&+t_{in}^{ab}\left(\frac{1}{2}t_{jm}^{cd}u_{cd}^{mn}\right)P(ij)\\
&-t_{ij}^{bd}\left(\frac{1}{2}t_{nm}^{ac}u_{cd}^{nm}\right)P(ab)\\
&+t_{im}^{ac}\left(\frac{1}{2}t_{jn}^{bd}u_{cd}^{mn}+u_{jc}^{bm}\right)P(ab)P(ij)\\
&+\frac{1}{2}t_{im}^{ab}u_{jn}^{mn}.
\end{aligned}
\tag{C4}
$$

Now we can introduce the intermediate χ-terms,

$$
\chi_{cd}^{ab}=\frac{1}{4}t_{mn}^{ab}u_{cd}^{mn}+\frac{1}{2}u_{cd}^{ab}
\tag{C5}
$$

$$
\chi_j^n=\frac{1}{2}t_{jm}^{cd}u_{cd}^{mn}
\tag{C6}
$$

$$
\chi_d^a=\frac{1}{2}t_{nm}^{ac}u_{cd}^{nm}
\tag{C7}
$$

$$
\chi_{jc}^{bm}=\frac{1}{2}t_{jn}^{bd}u_{cd}^{mn}+u_{jc}^{bm},
\tag{C8}
$$

this gives us,

$$
\begin{aligned}
0=&u_{ij}^{ab}+\tilde{f}_c^bt_{ij}^{ac}P(ab)-\tilde{f}_j^kt_{ik}^{ab}P(ij)\\
&+t_{ij}^{cd}\chi_{cd}^{ab}+t_{in}^{ab}\chi_j^nP(ij)-t_{ij}^{bd}\chi_d^aP(ab)\\
&+t_{im}^{ac}\chi_{jc}^{bm}P(ab)P(ij)+\frac{1}{2}t_{im}^{ab}u_{jn}^{mn}.
\end{aligned}
\tag{C9}
$$

Appendix D: Example Script

```python
from coupled_cluster.schemes.ccd_sparse import CoupledClusterDoublesSparse
from coupled_cluster.schemes.ccd_optimized import CoupledClusterDoublesOptimized
from coupled_cluster.hartree_fock.scf_rhf import scf_rhf
from coupled_cluster.matrix_elements.generate_matrices import (
    get_one_body_elements, get_coulomb_elements,
    get_antisymmetrized_elements, add_spin_to_one_body_elements,
    get_one_body_elements_spin
)
from coupled_cluster.matrix_elements.index_map import (
    generate_index_map, IndexMap
)
from coupled_cluster.hartree_fock.basis_transformation import (
    transform_one_body_elements, transform_two_body_elements
)

import numpy as np
import time
import os

file_path = os.path.join("..", "dat")
filename = os.path.join(file_path, "coulomb_{0}.pkl")

num_shells = 12
generate_index_map(num_shells)

omega = 2.0
l = IndexMap.shell_arr[-1]
n = 12
theta_hf = 0.1
theta_ho = 0.1
max_iterations = 1000

filename = filename.format(l)

print ("""
w = {0},
num_shells = {1},
l = {2},
n = {3},
theta_hf = {4},
theta_ho = {5},
filename = {6}
""".format(omega, num_shells, l, n, theta_hf, theta_ho, filename))

h = omega * get_one_body_elements(l)
t0 = time.time()
u = np.sqrt(omega) * get_coulomb_elements(l, filename=filename, tol=1e-12)
t1 = time.time()
print ("Time spent creating Coulomb elements: {0} sec".format(t1 - t0))

t0 = time.time()
c, energy = scf_rhf(h.todense(), u, np.eye(l//2), n//2, tol=1e-6)
t1 = time.time()
print ("Time spent in SCF RHF: {0} sec".format(t1 - t0))
```

```python
print ("\tRHF Energy: {0:.6f}".format(energy))

hi = transform_one_body_elements(h, c)
t0 = time.time()
oi = transform_two_body_elements(u, c)
t1 = time.time()
print ("Time spent transforming two body elements: {0} sec".format(t1 - t0))

_h = add_spin_to_one_body_elements(hi, l)
t0 = time.time()
_u = get_antisymmetrized_elements(l, oi=oi, tol=1e-12)
t1 = time.time()
print ("Time spent antisymmetrizing two body elements: {0} sec".format(t1 - t0))

t0 = time.time()
ccd_hf_sparse = CoupledClusterDoublesSparse(_h, _u, n)
t1 = time.time()
print ("Time spent setting up CCD code with HF basis: {0} sec".format(t1 - t0))

t0 = time.time()
energy, iterations = ccd_hf_sparse.compute_energy(tol=1e-4, theta=theta)
t1 = time.time()
print ("Time spent computing CCD energy with HF basis: {0} sec".format(t1 - t0))
print ("\tCCD (HF) Energy: {0}\n\tIterations: {1}\n\tSecond/iteration: {2}".format(energy, iterations, (

t0 = time.time()
ccd_hf = CoupledClusterDoublesOptimized(
        _h.todense(), _u.todense(), n, parallel=False)
t1 = time.time()
print ("Time spent setting up CCD (opt, parallel) code with HF basis: {0} sec"
    .format(t1 - t0))

t0 = time.time()
energy, iterations = ccd_hf.compute_energy(
        tol=1e-6, theta=theta_hf, max_iterations=max_iterations)
t1 = time.time()
print ("Time spent computing CCD (opt, parallel) energy with HF basis: {0} sec"
   .format(t1 - t0))
print ("\tCCD (HF) Energy: {0:.6f}\n\tIterations: {1}\n\tSecond/iteration: {2}"
    .format(energy, iterations, (t1 - t0)/iterations))

__h = omega * get_one_body_elements_spin(l)
t0 = time.time()
__u = np.sqrt(omega) * get_antisymmetrized_elements(l, filename=filename)
t1 = time.time()
print ("Time spent getting antisymmetric two body elements: {0} sec".format(t1 - t0))

t0 = time.time()
ccd = CoupledClusterDoublesOptimized(__h.todense(), __u.todense(), n)
t1 = time.time()
print ("Time spent setting up CCD code with HO basis: {0} sec".format(t1 - t0))
t0 = time.time()
energy, iterations = ccd.compute_energy(
        theta=theta_ho, tol=1e-6, max_iterations=max_iterations)
t1 = time.time()
print ("Time spent computing CCD energy with HO basis: {0} sec".format(t1 - t0))
print ("\tCCD Energy: {0:.6f}\n\tIterations: {1}\n\tSecond/iteration: {2}"
    .format(energy, iterations, (t1 - t0)/iterations))
```

[1] M. Taut, Journal of Physics A: Mathematical and General **27**, 1045 (1994).

[2] S. M. Reimann and M. Manninen, Reviews of modern physics **74**, 1283 (2002).

[3] E. Anisimovas and A. Matulis, Journal of Physics: Condensed Matter **10**, 601 (1998).

[4] H. B. Schlegel and J. McDouall, in *Computational Advances in Organic Chemistry: Molecular Structure and Reactivity* (Springer, 1991) pp. 167–185.

[5] G. E. Scuseria, T. J. Lee, and H. F. Schaefer III, Chemical physics letters **130**, 236 (1986).

[6] M. P. Lohne, G. Hagen, M. Hjorth-Jensen, S. Kvaal, and F. Pederiva, Physical Review B **84**, 115302 (2011).

[7] M. P. Lohne, *Coupled-cluster studies of quantum dots*, Master's thesis (2010).

[8] T. D. Crawford and H. F. Schaefer, Reviews in Computational Chemistry, Volume 14 , 33 (2007).